

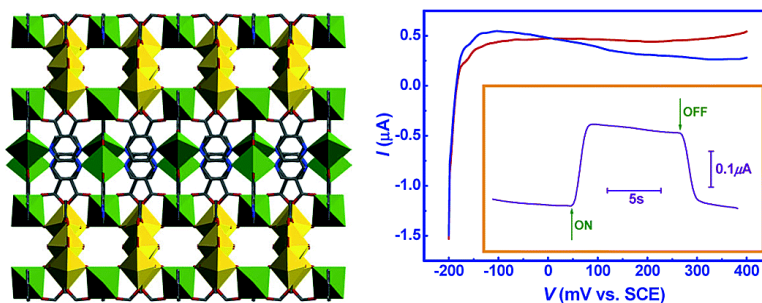
Communication

**Synthesis, Structure, and Photoelectronic Effects of a Uranium–Zinc–Organic Coordination Polymer Containing Infinite Metal Oxide Sheets**

Wei Chen, Hong-Ming Yuan, Jia-Yu Wang, Zhao-Yue Liu, Jin-Jie Xu, Min Yang, and Jie-Sheng Chen

*J. Am. Chem. Soc.*, **2003**, 125 (31), 9266-9267 • DOI: 10.1021/ja035388n • Publication Date (Web): 15 July 2003

Downloaded from <http://pubs.acs.org> on March 29, 2009



**More About This Article**

Additional resources and features associated with this article are available within the HTML version:

- Supporting Information
- Links to the 31 articles that cite this article, as of the time of this article download
- Access to high resolution figures
- Links to articles and content related to this article
- Copyright permission to reproduce figures and/or text from this article

[View the Full Text HTML](#)

## Synthesis, Structure, and Photoelectronic Effects of a Uranium–Zinc–Organic Coordination Polymer Containing Infinite Metal Oxide Sheets

Wei Chen, Hong-Ming Yuan, Jia-Yu Wang, Zhao-Yue Liu, Jin-Jie Xu, Min Yang, and Jie-Sheng Chen\*

State Key Laboratory of Inorganic Synthesis and Preparative Chemistry, College of Chemistry, Jilin University, Changchun 130023, P. R. China

Received March 31, 2003; E-mail: chemcj@mail.jlu.edu.cn

Actinide compounds display unusual structural complexity and variability, concomitant with a wide range of physicochemical properties that may find applications in fabrication of devices with optical,<sup>1</sup> magnetic,<sup>2</sup> and catalytic<sup>3</sup> properties. Thus far, considerable efforts have been devoted to the investigation of uranium-bearing materials,<sup>4</sup> such as uranyl oxide hydrates, phosphates, phosphonates, silicates, sulfides, sulfates, selenites, tellurites, iodates, fluorides, and molybdates. Metal–organic coordination polymers built up from U–O units, however, have not been examined, although uranium isonicotinates,<sup>4i</sup> in which the organic ligands do not bridge between inorganic units as in typical coordination polymers, were reported recently. In the present contribution, we describe  $(\text{ZnO})_2\text{-(UO}_2)_3(\text{NA})_4(\text{OAc})_2$  **1** (HNA = nicotinic acid; HOAc = acetic acid), a novel three-dimensional coordination polymer comprising inorganic U–O–Zn-clustered double sheets and organic ligands. Clustered metal–organic coordination polymers have been extensively studied in recent years, because the clustered metal ions often not only exhibit a variety of coordination advantages<sup>5</sup> but also introduce intriguing magnetic<sup>6</sup> and optoelectronic<sup>7</sup> properties. Thermal and photoelectrochemical analyses have been performed for our polymer compound, and the results indicate that it not only has a high thermal stability but also exhibits interesting photoelectronic properties.

In a typical hydrothermal synthesis,  $\text{ZnUO}_2(\text{OAc})_4 \cdot 7\text{H}_2\text{O}$  **2** (0.543 g, 0.5 mmol) was dissolved in water (15 mL). Pyridine-2,3-dicarboxylic acid (0.167 g, 1 mmol) and triethylamine (0.1 mL) were subsequently added to the solution. The final mixture was sealed in a Teflon-lined autoclave (20 mL) in air and heated at 160 °C for 3 days to give yellow crystals of **1** with ca. 59% yield based on uranium. It is interesting to note that decarboxylation occurred and the pyridine-2,3-dicarboxylic acid was transformed into NA in the process of the hydrothermal reaction. The IR spectrum shows one strong band at 914  $\text{cm}^{-1}$  for the asymmetric uranyl stretch,<sup>4c,d</sup> confirming the existence of uranyl groups. Phase purity of **1** is sustained by its powder X-ray diffraction pattern, which is consistent with that simulated on the basis of the single-crystal X-ray diffraction data. In addition, when we substituted the mixture of  $\text{Zn}(\text{OAc})_2 \cdot 4\text{H}_2\text{O}$  and  $\text{UO}_2(\text{OAc})_2 \cdot 2\text{H}_2\text{O}$  for **2** or replaced 2,3-dicarboxylic acid with HNA under the same synthetic conditions, compound **1** also formed, but the product was polycrystalline and was not suitable for single-crystal structure analysis.

X-ray single-crystal diffraction analysis<sup>8</sup> reveals that the structure of **1** possesses a three-dimensional structure with rich coordinations, including eight-coordinate hexagonal bipyramidal U(1) cations, seven-coordinate pentagonal bipyramidal U(2) cations, six-coordinate octahedral Zn(1) cations, and five-coordinate trigonal bipyramidal Zn(2) cations (Figure 1). Each uranium is axially

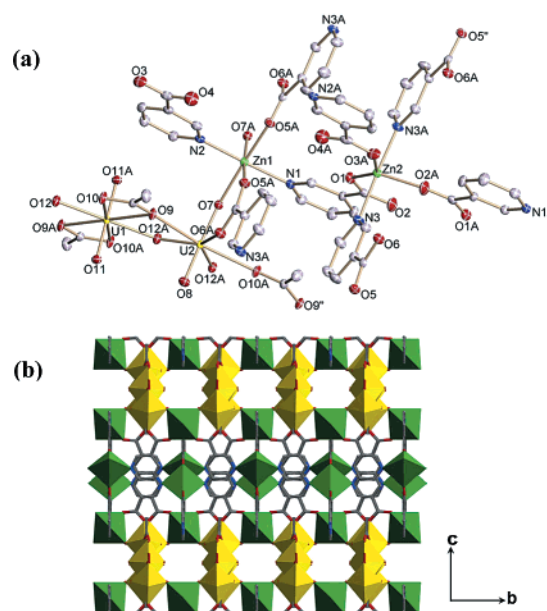


**Figure 1.** The structure of **1**: (a) the Zn and U coordination environment represented by thermal ellipsoids drawn to encompass 30% of their electron density; (b) the three-dimensional framework viewed along the [100] direction. Green:  $\text{ZnO}_5$  or  $\text{ZnO}_6$  units; yellow:  $\text{UO}_7$  or  $\text{UO}_8$  units.

bonded to two oxygens, forming a uranyl unit. Equatorially, U(1) and U(2) are separately bonded to five and six oxygens, with U–O bonds ranging from 2.231(4) to 2.628(5) Å, of which  $\mu_3$ -O(12) bridges to the adjacent edge-sharing uranyl units to form infinite straight U–O chains running along the *a* axis. Moreover, each acetate simultaneously chelates to one U(1) cation and bridges to two neighboring U(2) cations, riding on a U–O chain. These chains are corner-linked by Zn(1) cations via the uranyl oxygens (O(7)), leading to the topology of a robust inorganic U–O–Zn double sheet. These inorganic double sheets are further interconnected via Zn(1) and O(6) by the metal–organic layers resulting from the cross-linkage of zinc ions and tridentate NA ligands to construct a three-dimensional sandwich uranium–zinc–organic polymeric network (Figure 1b).

Thermogravimetric analysis (TGA) under an atmospheric environment shows no weight loss between room temperature and 400 °C, which is an indication of stability up to 400 °C. The high thermal stability of **1** is mainly attributed to the formation of U–O–Zn double layers that solidifies the flexible organic ligands. After thermal treatment at 600 °C for 4 h, the residue of **1** mainly consists of  $\text{ZnU}_3\text{O}_{10}$ , and a tiny amount of unknown phase is also present on the basis of powder X-ray diffraction.

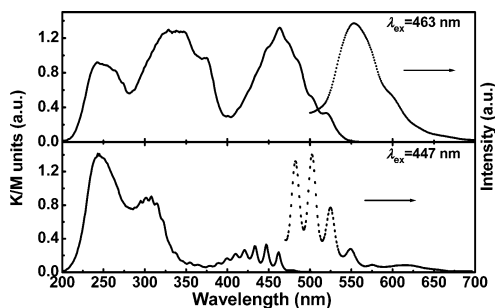


**Figure 2.** Diffuse reflectance UV-vis spectra (solid line) and solid-state emission spectra (dotted line) for **1** (top) and **2** (bottom) at room temperature.

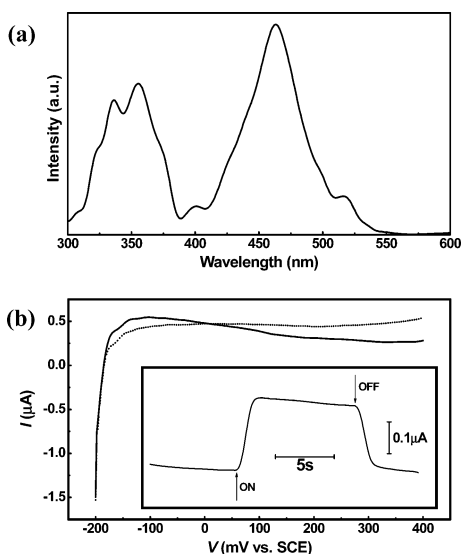


**Figure 3.** (a) SPS of polycrystalline **1**. (b) Linear voltammograms of ITO-polycrystalline **1** electrode in 0.1 mol/L  $\text{Na}_2\text{SO}_4$  solution under dark (solid lines) and illumination (dotted line) with cool white light. (Inset) Transient photocurrent response of ITO-**1** polycrystalline electrode at 0.4 V vs SCE. Arrows  $\uparrow$  and  $\downarrow$  indicate when light was turned on and off, respectively.)

The diffuse reflectance UV-vis spectra for **1** and **2** show different absorption features (Figure 2). There are three transitions at approximately 243, 310, and 440 nm for **2**. The transition at 440 nm, which is characteristic of uranyl absorptions,<sup>4e,9</sup> contains fine structure with about 14-nm separations. In contrast to the absorptions of **2**, the absorption spectrum of **1** gives a strong absorption peak at 463 nm. The transition at 243 nm for **1** remains the same in energy, whereas the other band shifts from 310 to 350 nm. As is well known, most uranyl-containing compounds emit green light,<sup>1</sup> and the source compound **2** also shows typical emission features for uranyl compounds with fine structure present when irradiated with 447-nm light. The emission spectrum for **1**, however, shows a main peak at 553 nm without fine structure.

By analogy with other metal oxide semiconductors (e.g. ZnO), **1** may be regarded as a two-dimensional semiconductor with its valence band consisting of the occupied O orbitals, whereas its conduction band consists of the empty metal orbitals. The nicotinate ligand should not contribute to the semiconducting nature of **1** because the diffuse reflectance UV-vis spectrum for nicotinic acid shows an absorption band below 300 nm whose wavelength is far shorter than that of the characteristic band for **1** at 463 nm. Under illumination without external electric field, the signal of surface photovoltage spectrum (SPS) for **1** (Figure 3a) shows two main response bands at approximately 350 and 463 nm, in accordance with the diffuse reflectance UV-vis spectrum. Furthermore, photoexcitation of the ITO-polycrystalline **1** electrode in a 0.1 mol/L

$\text{Na}_2\text{SO}_4$  solution causes generation of an anodic photocurrent. Figure 3b shows the change in linear voltammograms as a result of shuttering and unshuttering the light source. Under illumination, the photocurrent increases with anodic potential as commonly observed in an n-type semiconductor.<sup>10</sup> The transient photocurrent responses of **1** were recorded for several on-off cycles of illumination. In the inset of Figure 3b, a representative trace shows that an anodic photocurrent of ca.  $0.2 \mu\text{A}$  at constant 0.4 V applied voltage versus SCE was generated. The low photocurrent density in combination with a low electrical conductivity ( $<10^{-5} \text{ S cm}^{-1}$ ) for **1** suggests that this coordination polymer compound contains controlled carrier density, in contrast with conventional oxide semiconductors such as ZnO in which the carrier density is difficult to control down.<sup>11</sup> Compounds with a controlled carrier density may be favorable for fabrication of devices such as field effect transistors.<sup>11</sup> The successful synthesis of **1** and the finding of its unusual physical properties may also help to explore new types of semiconducting materials, especially among coordination polymer compounds containing actinides.

**Acknowledgment.** We thank the National Natural Science Foundation of China and the Education Ministry of China for financial support.

**Supporting Information Available:** Tables of fractional atomic coordinates, anisotropic thermal parameters, and bond distances and angles for **1**. Two stacking structures, IR spectrum, TGA curve, powder X-ray diffraction patterns and X-ray crystallographic file (CIF). This material is available free of charge via the Internet at <http://pubs.acs.org>.

## References

- Bean, A. C.; Peper, S. M.; Albrecht-Schmitt, T. E. *Chem. Mater.* **2001**, *13*, 1266–1272.
- Francis, R. J.; Halasyamani, P. S.; O'Hare, D. *Angew. Chem., Int. Ed.* **1998**, *37*, 2214–2217.
- Hutchings, G. J.; Heneghan, C. S.; Hundson, I. D.; Taylor, S. H. *Nature* **1996**, *384*, 341–343.
- (a) Wang, X. Q.; Huang, J.; Jacobson, A. J. *J. Am. Chem. Soc.* **2002**, *124*, 15190–15191. (b) Sutorik, A. C.; Kanatzidis, M. G. *J. Am. Chem. Soc.* **1997**, *119*, 7901–7902. (c) Norquist, A. J.; Thomas, P. M.; Doran, M. B.; O'Hare, D. *Chem. Mater.* **2002**, *14*, 5179–5184. (d) Norquist, A. J.; Thomas, P. M.; Boran, M. B.; O'Hare, D. *Dalton Trans.* **2003**, 1168–1175. (e) Almond, P. M.; Albrecht-Schmitt, T. E. *Inorg. Chem.* **2002**, *41*, 1177–1183. (f) Almond, P. M.; McKee, M. L.; Albrecht-Schmitt, T. E. *Angew. Chem., Int. Ed.* **2002**, *41*, 3426–3429. (g) Bean, A. C.; Campana, C. F.; Kwon, O.; Albrecht-Schmitt, T. E. *J. Am. Chem. Soc.* **2001**, *123*, 8806–8810. (h) Halasyamani, P. S.; Walker, S. M.; O'Hare, D. *J. Am. Chem. Soc.* **1999**, *121*, 7415–7416. (i) Kim, J.-Y.; Norquist, A. J.; O'Hare, D. *Chem. Mater.* **2003**, *15*, 1970–1975.
- (a) Li, H. L.; Eddaoudi, M.; O'Keeffe, M.; Yaghi, O. M. *Nature* **1999**, *402*, 276–279. (b) Chui, S. S.-Y.; Lo, S. M.-F.; Charmant, J. P. H.; Orpen, A. G.; Williams, I. D. *Science* **1999**, *283*, 1148–1150. (c) Chen, B. L.; Eddaoudi, M.; Hyde, S. T.; O'Keeffe, M.; Yaghi, O. M. *Science* **2001**, *291*, 1021–1023.
- Chen, W.; Yue, Q.; Chen, C.; Yuan, H. M.; Xu, W.; Chen, J. S.; Wang, S. N. *Dalton Trans.* **2003**, 28–30.
- Chen, W.; Wang, J. Y.; Chen, C.; Yue, Q.; Yuan, H. M.; Chen, J. S.; Wang, S. N. *Inorg. Chem.* **2003**, *42*, 944–946.
- Crystal data: size = 0.20 mm  $\times$  0.10 mm  $\times$  0.08 mm; formula,  $\text{C}_{14}\text{H}_{11}\text{N}_2\text{O}_{10}\text{U}_{1.5}\text{Zn}$ ; MW, 789.66; monoclinic, space group  $C2/m$  (No. 12); cell dimensions  $a = 14.1221(6) \text{ \AA}$ ,  $b = 14.6697(6) \text{ \AA}$ ,  $c = 17.6379(8) \text{ \AA}$ ,  $\beta = 100.274(2)^\circ$ ,  $V = 3595.4(3) \text{ \AA}^3$ ,  $Z = 8$ ,  $\rho_{\text{calcd}} = 2.918 \text{ g cm}^{-3}$ ,  $\mu = 14.873 \text{ mm}^{-1}$ ,  $T = 293(2) \text{ K}$ . A total of 14104 reflections were collected, of which 5171 were independent reflections [ $R_{\text{int}} = 0.0408$ ]. Final  $R$  indices [ $I > 2\sigma(I)$ ]:  $R_1 = 0.0284$ ,  $wR_2 = 0.0574$ ,  $\text{GOF} = 0.992$ . Maximum and minimum residual electron density are 2.027 and  $-1.645 \text{ e} \cdot \text{\AA}^{-3}$ . Elemental anal.: Exp. (Calcd) C, 21.30 (21.29); N 1.56 (1.40); H 3.55 (3.55).
- Volkovich, V. A.; Griffiths, T. R.; Fray, D. J.; Thied, R. C. *Phys. Chem. Chem. Phys.* **2001**, *3*, 5182–5191.
- (a) Schneemeyer, L. F.; Wrighton, M. S. *J. Am. Chem. Soc.* **1979**, *101*, 6496–6500. (b) Qian, X. M.; Qin, D. Q.; Song, Q.; Bai, Y. B.; Li, T. J.; Tang, X. Y.; Wang, E. K.; Dong, S. J. *Thin Solid Films* **2001**, *385*, 152–161.
- Nomura, K.; Ohta, H.; Ueda, K.; Kamiya, T.; Hirano, M.; Hosono, H. *Science* **2003**, *300*, 1269–1272.

JA035388N